Letter

Josephson quantum mechanics at odd parity

Manuel Houzet and Julia S. Meyer
Univ. Grenoble Alpes, CEA, Grenoble INP, IRIG, Pheliqs, 38000 Grenoble, France

Yuli V. Nazarov
Kavli Institute of Nanoscience, Delft University of Technology, 2628 CJ Delft, The Netherlands

(Received 6 September 2023; revised 7 March 2024; accepted 15 July 2024; published 29 July 2024)

A Josephson junction may be in a stable odd-parity state when a single quasiparticle is trapped in an Andreev bound state. Embedding such junction in an electromagnetic environment gives rise to a special quantum mechanics of the superconducting phase that we investigate theoretically. Our analysis covers several representative cases, from the lifting of the supercurrent quench due to quasiparticle poisoning for a low ohmic impedance of the environment, to a Schmid transition in a current-biased junction that for odd parity occurs at four times bigger critical impedance. For intermediate impedances, the supercurrent in the odd state is higher than in the even one.

DOI: 10.1103/PhysRevB.110.L020504

Introduction. The energy of a tunnel junction between two superconducting leads depends periodically on the difference of superconducting phases of the two, in short, on the phase. This is the celebrated Josephson effect [1]: The phase dependence of this energy gives rise to a persistent superconducting current between the leads. Later, it has been understood that the phase becomes a quantum-fluctuating variable if a Josephson junction is embedded in an electromagnetic circuit [2]. Early studies concentrated on a dissipative environment and were essential for establishing the modern theory of dissipative quantum mechanics [3,4]. A highlight of this research was the prediction of the Schmid transition [5]: the vanishing of the Josephson energy at a critical value of the circuit impedance R, $2e^2R/\pi\hbar \equiv \alpha = 1$. While this prediction is theoretically indisputable, the controversy concerning its experimental verification [6,7] may have been resolved recently [8]. The further development of Josephson quantum mechanics evolved from dissipative circuits to dissipationless Coulomb islands. The resulting superconducting qubits [9,10] are at the frontline of modern quantum technology applications.

There is something to add to this well-established field. In fact, the Josephson energy is related to Andreev bound states (ABS) in the junction [11] and does depend on their occupation. Of the two equal-weight superpositions with respect to the right/left leads in which a quasiparticle may be in, only one gives rise to a bound state. Owing to parity conservation in superconductors [12], a state with a single quasiparticle trapped in the lowest ABS (the odd-parity ground state) is stable despite having a bigger energy than the state without quasiparticles (the even-parity ground state) [13]. The parity can only be relaxed if a stray quasiparticle from a lead comes to the junction and annihilates the trapped one. Since the concentration of quasiparticles in the leads is vanishingly small at low temperatures, the lifetime of the odd-parity ground state is macroscopically long: Lifetimes of several minutes have been measured [14]. Moreover, a single quasiparticle trapped in a spin-degenerate ABS eventually quenches the contribution of this level to the Josephson energy: This is called quasiparticle poisoning and has been observed in Ref. [15]. When spin degeneracy is lifted, the stability of these odd states provided the opportunity for a new kind of qubits: Andreev spin qubits, proposed in Refs. [16,17] and realized in Ref. [18]. In recent years, there has been an outburst of studies of ABS in superconducting nanostructures, including spectroscopically resolved ABS and odd-parity ground states in a junction [19]. This makes it relevant to extend the Josephson quantum mechanics to the case of a circuit embedding a Josephson junction in the odd-parity ground state.

Summary of results. In this Letter, we provide a general description of Josephson quantum mechanics at odd parity by considering a tunnel junction where the ABS are close to the superconducting gap Δ, disregarding the weak spin-orbit interaction, and mainly concentrating on the instructive single-channel, single-junction case (see Fig. 1). In particular, our setup does not include any quantum dot, nor does it involve Coulomb blockade physics. The main difference with the even-parity case stems from the coupling to the electromagnetic environment by one-electron rather than Cooper pair transfers.

We also present a detailed analysis for three relevant cases. (i) For low ohmic impedance, we demonstrate the incompleteness of supercurrent quenching and reveal a supercurrent jump at zero phase. We ascribe this jump to the quantum fluctuations of the phase, which extend the phase interval where the ABS in a given (right or left) superposition exists beyond 2π, such that two ABS of opposite superpositions coexist in the vicinity of phases that are multiples of 2π. The current jump then results from the cusp in the energy of the odd-parity ground state, when ABS cross each other. (ii) For arbitrary ohmic impedance and *phase* bias, we establish a slower suppression of the Josephson energy in the odd state

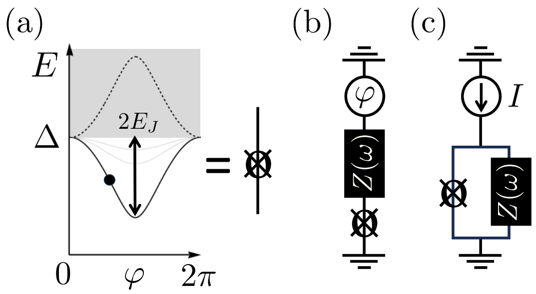

FIG. 1. (a) The odd-parity Josephson junction. A single quasiparticle is trapped in the lowest Andreev level separated by $2E_J \sin^2 \frac{\varphi}{2} \ll \Delta$ from the edge of the continuous quasiparticle spectrum at the superconducting energy gap Δ. In the bound state, the quasiparticle is in a certain superposition, $s = 1$, and the antibound state corresponding to $s = -1$ (dashed curve) belongs to the continuous spectrum. (b), (c) The Josephson quantum mechanics at odd parity: The odd-parity Josephson junction is embedded in a linear electromagnetic environment with frequency-dependent impedance $Z(\omega)$ that causes quantum fluctuations of the phase. (b) and (c) correspond to phase and current bias, respectively.

than in the even one: The supercurrent in the odd state thus becomes *higher* than in the even one, both remaining finite at any α (as already shown in the even case [20]). At sufficiently large impedance, *both* right/left superpositions form a bound state. While their phase dependence is suppressed upon increasing the impedance, their average binding energy tends to a constant. (iii) For arbitrary ohmic impedance and *current* bias, we encounter a Schmid transition at a higher value of the impedance than in the even state, namely, at $\alpha = 4$. The bound states persist for both superpositions and are *degenerate* for $\alpha > 4$. These predictions can be tested in forthcoming experiments.

Coupling an ABS with an electromagnetic environment. Let us sketch the general derivation before discussing our results for the three cases listed above: All details are provided in the Supplemental Material (SM) [21]. At even parity, the Hamiltonian describing a Josephson junction embedded in a general linear environment reads [22]

$$H_\mathrm{e} = H_\mathrm{env} - E_J^* \cos \hat{\varphi}. \tag{1}$$

Here, H_env is a Hamiltonian of noninteracting bosons, the operator of the phase drop at the junction, $\hat{\varphi}$, consists of the phase bias φ and a linear superposition of environmental bosons reproducing the frequency-dependent impedance of the environment, $Z(\omega)$, which is assumed to vanish above a frequency scale $\ll\Delta$, and E_J^* is the even-state Josephson energy. An alternative description [23] employs a path integral over a variable $\varphi(\tau)$ defined in imaginary time. The action that defines the path weight reads

$$\mathcal{S} = \sum_\omega \frac{|\omega|}{8e^2 Z(i|\omega|)} |\varphi(\omega)|^2 - E_J^* \int d\tau \cos \varphi(\tau), \tag{2}$$

$\varphi(\omega)$ being the Fourier transform of $\varphi(\tau)$.

To describe the odd-parity situation, we rely on the small junction transparency to consider the combined Fock space for one quasiparticle with energy (counted from the energy $E_g^{(e)}$ of the even-parity ground state) close to Δ, which can tunnel between the leads, and the environmental degrees of freedom. We then integrate out the quasiparticle degree of freedom for the purpose of finding a closed equation obeyed by the wave function $|\Phi\rangle$ of the environment. At vanishing impedance, this gives the binding energy Ω, measured from the edge of the continuum, in the following form (see Sec. I of SM [21]):

$$\sqrt{\Omega} = s\sqrt{2E_J} \sin \frac{\varphi}{2}. \tag{3}$$

Here, E_J is the Josephson energy associated with the lowest ABS: $E_J = E_J^*$ in the single-channel case, $E_J^* > E_J$ in general, and $s = \pm 1$ characterizes the superposition between right/left leads. Equation (3) with $s = \mathrm{sgn}(\sin \frac{\varphi}{2})$ reproduces the ABS dispersion in a short junction in the tunnel limit [24]. With the environment, the quantum generalization of Eq. (3), derived in Sec. II of SM [21], yields a singular-value equation that involves *square roots* of Hamiltonian-like operators,

$$\left(\sqrt{\Omega + H} - s\sqrt{2E_J} \sin \frac{\hat{\varphi}}{2}\right)|\Phi\rangle = 0, \tag{4}$$

where $H = H_\mathrm{e} - E_g^{(e)}$. In addition, the energy of the odd-parity ground state is $E_g^{(o)} = E_g^{(e)} + \Delta - \Omega$.

The solution Ω of Eq. (4) can be found as the pole of a propagator associated with the quantum dynamics described by its left-hand side. As Eq. (4) contains the same environmental degrees of freedom as in the even sector, we make use of the imaginary-time action, Eq. (2), to define the appropriate propagator through the Dyson equation that it solves,

$$G(\tau, \tau') = G_0(\tau - \tau') + \int d\tau_1 G_0(\tau - \tau_1) A(\tau_1) G(\tau_1, \tau'). \tag{5}$$

Here, $G_0(\tau) \equiv \Theta(\tau)/\sqrt{\pi\tau}$, corresponding to the first (square-root) term in Eq. (4), is the bare propagator that arises from integrating out quasiparticles. The second term in Eq. (4) is treated in all orders, similarly as in the Green's function treatment of a frozen disorder [25], by introducing $A(\tau) \equiv s\sqrt{2E_J} \sin \frac{\varphi(\tau)}{2}$ that plays the role of the disorder potential. Ultimately, the disorder averaging is done with the weight $e^{-\mathcal{S}}$ (see Sec. III in SM [21]). The averaged propagator (denoted with a bar) is uniform, so its Fourier components read

$$\bar{G}(\omega) = [\sqrt{i\omega} - \langle A \rangle - \Sigma(\omega)]^{-1}, \tag{6}$$

the self-energy $\Sigma(\omega)$ being a sum of diagrams involving the correlators of $A(\tau)$ starting from the second order. Finally, the binding energy is found from

$$\sqrt{\Omega} = \langle A \rangle + \Sigma(-i\Omega). \tag{7}$$

Equations (4) and (7) hold for an arbitrary linear environment. Below we use them to make specific predictions in the case of a dissipative environment.

Small ohmic impedance. Let us start with the case of small ohmic impedance, $\alpha \ll 1$. For a concrete model, we add a capacitance and an inductance in parallel to the resistor R. This cuts the ohmic response both at high and low frequency, $\omega_H = 1/RC$ (with $\omega_H \ll \Delta$) and $\omega_L = R/L$, respectively. The inductance is required in order to phase bias the junction, $E_J e^2 L \ll 1$. We concentrate on the single-channel case: $E_g^{(o)}$ does not depend on phase without fluctuations. We aim to compute

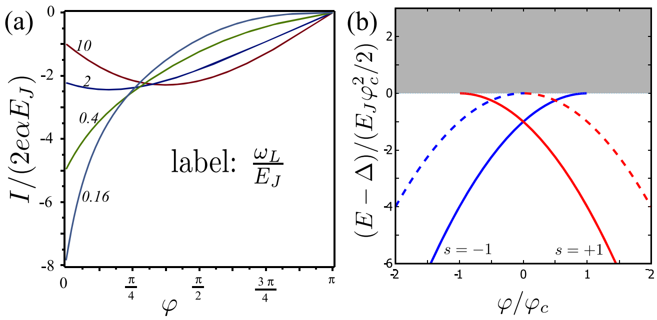

FIG. 2. (a) The odd-parity supercurrent at small impedance. The curve labels are ω_L/E_J, so we set $\ln(\omega_H/\omega_L) = 5$. (b) Bound states near zero phase for $s = \pm 1$. Here, $\varphi_c = \pi\alpha\sqrt{E_J/\omega_L} \ll 1$. Dashed curves: No interaction.

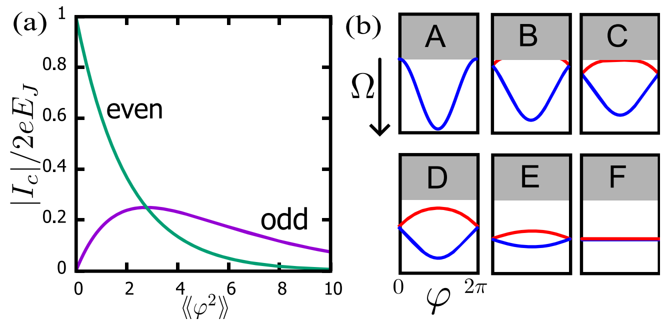

FIG. 3. (a) Critical currents at even and odd parity vs $\langle\langle\varphi^2\rangle\rangle$, Eq. (12). The odd-parity current dominates at $\langle\langle\varphi^2\rangle\rangle > 4\ln 2 \approx 2.8$. (b) The bound regimes in the odd-parity Josephson junction. A: Only one superposition gives rise to a bound state ($\alpha = 0$). B: Two bound states in a finite phase interval [cf. Fig. 2(b)]. C: Separatrix between B and D. D: Two 4π-periodic bound states are present at all phases. E: The splitting of the two bound states is much smaller than their average phase-independent energy. F: The two states $s = \pm 1$ with phase-independent energy are degenerate.

the phase-dependent correction $\delta E_g^{(o)}(\varphi)$ proportional to the fluctuations, which defines the supercurrent in the odd state.

A simple *ad hoc* estimation would be $\delta E_g^{(o)} \simeq \alpha E_J \cos\varphi$. While this may be a correct scale, the answer is more involved and interesting [see Fig. 2(a)]. We note an extra dimensionless parameter ω_L/E_J that can be large or small provided $\alpha \ll 1$. We see that the current in the phase interval $\varphi \in [0, \pi]$ is *negative*: The minimum odd-parity Josephson junction energy corresponds to $\varphi = \pi$ rather than $\varphi = 0$. Let us note that this π-junction behavior has a completely different origin than the one induced by magnetic correlations [26] or a finite length of the junction [27]. At $\omega_L \gg E_J$,

$$\frac{I(\varphi)}{2e} = -\frac{\alpha E_J}{2}\ln\left(\frac{\omega_H}{\omega_L}\right)\sin\varphi \tag{8}$$

holds under the stronger condition $\alpha \ll 1/\ln(\omega_H/\omega_L)$; the log factor is a precursor of the renormalization of E_J at $\alpha \sim 1$ [see Eq. (11)]. The most interesting feature present for arbitrary ratios ω_L/E_J is the current jump at $\varphi = 0$, its half value being $I_{\rm hj} = -2\pi\alpha e E_J\sqrt{E_J/\omega_L}$. At $\omega_L \ll E_J$, the supercurrent is concentrated at small $\varphi \simeq \sqrt{\omega_L/E_J}$ and reads $I(\varphi) = -|I_{\rm hj}| f(\varphi/\sqrt{2\omega_L/E_J})$ with $f(0) = 1$ and $f(x) \to \sqrt{2}/\pi x$ at $x \to \infty$. The full expression for the monotonous function $f(x)$ is given in Sec. IV of SM [21].

The current jump is associated with the fact that perturbation theory formally ceases to hold at small φ. However, the answer beyond perturbations is really simple and shown in Fig. 2(b): Namely the binding energy is shifted such that the bound state reaches the continuum edge not at $\varphi = 0$, but at $\varphi = -s\varphi_c$ with $\varphi_c \equiv (|I_{\rm hj}|/2e)/E_J$, i.e., the binding energy is given by $\sqrt{\Omega} = \sqrt{E_J/2}(s\varphi + \varphi_c)$. The shifts being opposite for $s = \pm 1$ implies the presence of bound states for *both* superpositions in an interval $|\varphi| < \varphi_c$: This fact will become crucial for further analysis. (A small gap asymmetry between the leads breaks the conservation of s and broadens the current jump; see Sec. VII in SM [21].)

Phase bias. Let us turn to the case of an arbitrary impedance, $\alpha \simeq 1$, under conditions of *phase bias*. In this case, the low cutoff frequency is such that $\omega_L \gg E_J$ and does not change upon renormalization of E_J, E_J^*. The renormalization is thus finite at any α: This implies that no Schmid transition occurs under phase bias. While $E_J = E_J^*$ in the single-channel case, they renormalize differently. The renormalization can be computed using the relation $\langle e^{i\beta\varphi}\rangle = e^{i\beta\langle\varphi\rangle}e^{-\beta^2\langle\langle\varphi^2\rangle\rangle/2}$, where $\langle\langle\varphi^2\rangle\rangle = \langle\varphi^2\rangle - \langle\varphi\rangle^2$, valid for Gaussian fluctuations of the phase. At even parity,

$$\tilde{E}_J^* = E_J^* e^{-\langle\langle\varphi^2\rangle\rangle/2} \simeq E_J^*(\omega_L/\omega_H)^\alpha. \tag{9}$$

Here and further on the "tilde" refers to renormalized quantities.

To understand the renormalization at odd parity, we keep terms up to the second order in the self-consistency equation (7),

$$\sqrt{\Omega} = \langle A\rangle + \Sigma^{(2)}(-i\Omega). \tag{10}$$

The average A is phase dependent and strongly suppressed,

$$\langle A\rangle = s\sqrt{2\tilde{E}_J}\sin\frac{\varphi}{2} \quad \text{with} \quad \frac{\tilde{E}_J}{E_J} = e^{-\frac{\langle\langle\varphi^2\rangle\rangle}{4}} \simeq \left(\frac{\omega_L}{\omega_H}\right)^{\frac{\alpha}{2}}. \tag{11}$$

The suppression of E_J is two times weaker than the one of E_J^* in Eq. (9) for even parity. At $\alpha < 1$ we can ignore $\Sigma^{(2)}$ (see below). As the odd-parity energy is the difference of even-parity and binding energies, with the renormalized Josephson couplings of Eqs. (9) and (11), respectively, the superconducting current in the odd state reads

$$\frac{I(\varphi)}{2e} = (\tilde{E}_J^* - \tilde{E}_J)\sin\varphi = E_J\big(e^{-\frac{\langle\langle\varphi^2\rangle\rangle}{2}} - e^{-\frac{\langle\langle\varphi^2\rangle\rangle}{4}}\big)\sin\varphi \tag{12}$$

and is bigger than that at even parity at sufficiently large phase fluctuations [see Fig. 3(a)].

However, the second-order term $\Sigma^{(2)}(-i\Omega)$ can become important since it has a phase-independent part. This leads to a variety of *bound* regimes listed in Fig. 3(b). For estimates, we concentrate on the phase-independent terms in $\Sigma^{(2)}$ and, since $\Omega \ll \omega_L$, disregard the Ω dependence. This yields

$$\Sigma^{(2)} = E_J\int_0^\infty \frac{d\tau}{\sqrt{\pi\tau}}\langle\langle e^{i\varphi(0)/2}e^{-i\varphi(\tau)/2}\rangle\rangle. \tag{13}$$

The integrand at $\omega_H^{-1} \ll \tau \ll \omega_L^{-1}$ is proportional to $1/\tau^{1/2}(\omega_H\tau)^{\alpha/2}$. As a consequence, the integral converges at the lower cutoff if $\alpha < 1$ and at the upper cutoff if $\alpha > 1$. The estimations for $\Sigma^{(2)}$ thus read (see Sec. V in SM [21])

$$\Sigma^{(2)} \simeq \begin{cases} \tilde{E}_J/\sqrt{\omega_L}, & 1-\alpha \gg 1/\ln(\omega_H/\omega_L), \\ E_J/\sqrt{\omega_H}, & \alpha - 1 \gg 1/\ln(\omega_H/\omega_L). \end{cases} \quad (14)$$

Comparing $\langle A \rangle$ at $\varphi = \pi$ and $\Sigma^{(2)}$, we observe that the latter dominates for $\alpha > 2[1 + \ln(\omega_L/E_J)/\ln(\omega_H/\omega_L)] \equiv \alpha_c > 2$. This point separates two different regimes. Now we can summarize the results.

At $\alpha < \alpha_c$, $\Sigma^{(2)}$ can be neglected in zeroth approximation. The superconducting current is given by Eq. (12). Starting from the case without fluctuations (regime A), we find that the addition of small phase-independent terms in Eq. (10) when fluctuations are weak leads to the coexistence of two bound states corresponding to the two superpositions $s = \pm 1$ in a small interval of phases around $\varphi = 0$ (regime B). At $\alpha > 1$, this interval grows with increasing α until an important transition (regime C) takes place at α_c: Two bound states are present at any phase. For $\alpha > \alpha_c$, both bound states are separated from the continuum by a gap (regime D). Thus the odd-parity state becomes stable upon an adiabatic sweep of the phase. The bound energies are given by

$$\Omega = \left(s\sqrt{2\tilde{E}_J}\sin\frac{\varphi}{2} + \Sigma^{(2)}\right)^2. \quad (15)$$

The resulting superconducting current at a given s thus becomes 4π periodic, a phenomenon similar to that signifying the presence of Majorana modes [28].

At α slightly [by $\simeq 1/\ln(\omega_H/\omega_L) \ll 1$] exceeding α_c, the binding energy $\Omega \simeq E_J^2/\omega_H \gg \tilde{E}_J$ hardly depends on the phase and α (regime E). The remaining phase dependence results in a strongly suppressed 4π-periodic supercurrent,

$$\frac{I(\varphi)}{2e} \simeq s\tilde{E}_J^{\rm eff}\cos\frac{\varphi}{2}, \quad \tilde{E}_J^{\rm eff} \simeq \sqrt{\tilde{E}_J\Omega} \simeq E_J\sqrt{\frac{\tilde{E}_J}{\omega_H}}. \quad (16)$$

Despite being suppressed, this supercurrent parametrically exceeds the one at even parity [see Fig. 4(a)].

Current bias. Let us now turn to the case of an arbitrary impedance at *current bias*. In contrast with the phase bias situation, there is no built-in low-energy cutoff ω_L: The renormalization has to be cut off self-consistently by the renormalized Josephson energy.

Let us first reproduce the Schmid transition at even parity. The renormalized $\tilde{E}_J^*$ is given by the same Eq. (9), yet ω_L there has to be estimated as $\tilde{E}_J^*$. With this,

$$\frac{\tilde{E}_J^*}{E_J^*} = \left(\frac{E_J^*}{\omega_H}\right)^{\frac{\alpha}{1-\alpha}}, \quad (17)$$

such that $\tilde{E}_J^*$ vanishes at the Schmid transition, $\alpha = 1$.

Let us next turn to the odd-parity sector. To start with, let us concentrate on the interval $\alpha < 1$. In this case, the lower cutoff can be unambiguously identified as $\tilde{E}_J$. Applying Eq. (11), we thus obtain

$$\frac{\tilde{E}_J}{E_J} = \left(\frac{E_J}{\omega_H}\right)^{\frac{\alpha}{2-\alpha}}. \quad (18)$$

The estimation of $\Sigma^{(2)}$ with the help of Eq. (14) gives $\Sigma^{(2)} \simeq \sqrt{\tilde{E}_J}$. In contrast with the phase-biased case, the first- and second-order contributions are of the same order of

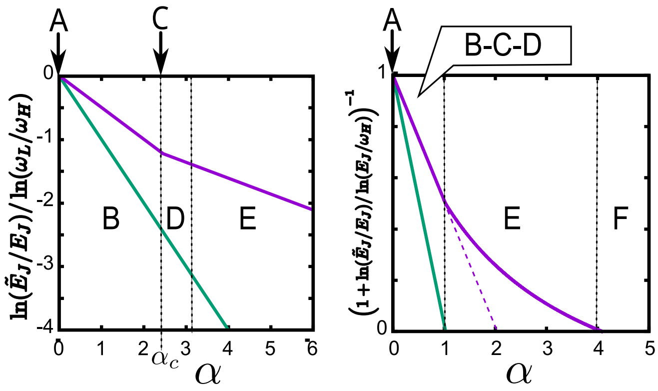

FIG. 4. Renormalized Josephson energies $\tilde{E}_J^*$ (green) at even and $\tilde{E}_J$ (violet) at odd parity. Vertical dotted lines separate the bound regimes at odd parity indicated by capital letters. Left: Phase bias [cf. Eqs. (9), (11), and (16)]; $\tilde{E}_J$ never vanishes. The separating regime C occurs at $\alpha = \alpha_c$. We plot $\tilde{E}_J^{\rm eff}$ instead of $\tilde{E}_J$ at $\alpha > \alpha_c$. Right: Current bias [cf. Eqs. (17)–(19)]; the curves illustrate the suppression of $\tilde{E}_J$ as α increases, and the Schmid transition where $\tilde{E}_J$ vanishes is at $\alpha = 1$ for even parity and at $\alpha = 4$ for odd parity. The renormalization law at odd parity changes at $\alpha = 1$. Note the different vertical scales in the left and right plot.

magnitude, as well as all higher orders. So in the current bias case, the accuracy of the method does not allow to predict the phase dependence of the energy, nor if bound states persist for both values of s (regimes B-C-D).

However, we still may notice and use the difference in the renormalizations of phase-dependent and phase-independent parts of $\sqrt{\Omega}$ depending on the value of α. This becomes important at $\alpha > 1$ where, in accordance with Eq. (14), the self-energy $\Sigma^{(2)}$ no longer depends on the low-energy cutoff and saturates at the value $\simeq E_J/\sqrt{\omega_H}$. As to the phase-dependent part, it will further decrease with increasing α. This brings us to regime E: the almost degenerate bound state associated with the supercurrent described by Eq. (16). In this case, the renormalization of E_J is cut off by $\tilde{E}_J^{\rm eff}$ of Eq. (16), rather than $\tilde{E}_J$. This yields

$$\frac{\tilde{E}_J}{E_J} = \left(\frac{E_J}{\omega_H}\right)^{\frac{3\alpha}{4-\alpha}}, \quad \frac{\tilde{E}_J^{\rm eff}}{E_J} = \left(\frac{E_J}{\omega_H}\right)^{\frac{\alpha+2}{4-\alpha}}. \quad (19)$$

Therefore $\tilde{E}_J, \tilde{E}_J^{\rm eff}$ vanish at $\alpha = 4$ [see Fig. 4(b)]. This is the new Schmid transition point for half of the Cooper pair charge, indeed corresponding to 4π periodicity in phase of the supercurrent. At $\alpha > 4$, the phase-independent bound state is completely degenerate with respect to s (regime F). Recalling the quasiparticle spin, we thus predict the realization of fourfold degeneracy for the trapped quasiparticle.

Conclusion. We have formulated the Josephson quantum mechanics for a junction in the odd-parity state. We concentrated on the single-channel case and predicted the lifting of the supercurrent quench due to quasiparticle poisoning at small impedance. Furthermore, we have addressed the case of arbitrary impedance both at phase and current bias. The supercurrent at odd parity is less suppressed by quantum fluctuations and may dominate over the one at even parity. The presence of various bound regimes complicates the renormalization. For current bias, we predict a Schmid transition at $\alpha = 4$ and fourfold degenerate bound states at higher impedances. Quasiparticle poisoning is ubiquitous in Andreev devices. Therefore our results call for revisiting the role of the electromagnetic environment on the currently much studied Andreev and Majorana qubits.

Acknowledgments. Y.V.N. acknowledges support from the Université Grenoble Alpes for an extended stay in Grenoble during which most of the presented work was performed. M.H. and J.S.M. acknowledge funding from the Plan France 2030 through the Project NISQ2LSQ ANR-22-PETQ-0006 and FERBO ANR-23-CE47-0004.

[1] B. Josephson, Possible new effects in superconductive tunnelling, Phys. Lett. **1**, 251 (1962).
[2] A. J. Leggett, Macroscopic quantum systems and the quantum theory of measurement, Prog. Theor. Phys. Suppl. **69**, 80 (1980).
[3] A. J. Leggett, S. Chakravarty, A. T. Dorsey, M. P. A. Fisher, A. Garg, and W. Zwerger, Dynamics of the dissipative two-state system, Rev. Mod. Phys. **59**, 1 (1987).
[4] U. Weiss, *Quantum Dissipative Systems*, Series in Modern Condensed Matter Physics (World Scientific, Singapore, 1999).
[5] A. Schmid, Diffusion and localization in a dissipative quantum system, Phys. Rev. Lett. **51**, 1506 (1983).
[6] A. Murani, N. Bourlet, H. le Sueur, F. Portier, C. Altimiras, D. Esteve, H. Grabert, J. Stockburger, J. Ankerhold, and P. Joyez, Absence of a dissipative quantum phase transition in Josephson junctions, Phys. Rev. X **10**, 021003 (2020).
[7] D. Subero, O. Maillet, D. S. Golubev, G. Thomas, J. T. Peltonen, B. Karimi, M. Marín-Suárez, A. L. Yeyati, R. Sánchez, S. Park, and J. P. Pekola, Bolometric detection of coherent Josephson coupling in a highly dissipative environment, Nat. Commun. **14**, 7924 (2023).
[8] R. Kuzmin, N. Mehta, N. Grabon, R. A. Mencia, A. Burshtein, M. Goldstein, and V. E. Manucharyan, Observation of the Schmid-Bulgadaev dissipative quantum phase transition, arXiv:2304.05806.
[9] Y. Makhlin, G. Schön, and A. Shnirman, Quantum-state engineering with Josephson-junction devices, Rev. Mod. Phys. **73**, 357 (2001).
[10] A. Blais, A. L. Grimsmo, S. M. Girvin, and A. Wallraff, Circuit quantum electrodynamics, Rev. Mod. Phys. **93**, 025005 (2021).
[11] C. W. J. Beenakker, Universal limit of critical-current fluctuations in mesoscopic Josephson junctions, Phys. Rev. Lett. **67**, 3836 (1991).
[12] D. V. Averin and Y. V. Nazarov, Single-electron charging of a superconducting island, Phys. Rev. Lett. **69**, 1993 (1992).
[13] Here, we use the quasiparticle picture, where many-body states are formed of excitations with positive energies on top of the superconducting condensate.
[14] D. J. van Woerkom, A. Geresdi, and L. P. Kouwenhoven, One minute parity lifetime of a NbTiN Cooper-pair transistor, Nat. Phys. **11**, 547 (2015).
[15] M. Zgirski, L. Bretheau, Q. Le Masne, H. Pothier, D. Esteve, and C. Urbina, Evidence for long-lived quasiparticles trapped in superconducting point contacts, Phys. Rev. Lett. **106**, 257003 (2011).
[16] N. M. Chtchelkatchev and Y. V. Nazarov, Andreev quantum dots for spin manipulation, Phys. Rev. Lett. **90**, 226806 (2003).
[17] C. Padurariu and Y. V. Nazarov, Theoretical proposal for superconducting spin qubits, Phys. Rev. B **81**, 144519 (2010).
[18] M. Hays, V. Fatemi, D. Bouman, J. Cerrillo, S. Diamond, K. Serniak, T. Connolly, P. Krogstrup, J. Nygård, A. L. Yeyati, A. Geresdi, and M. H. Devoret, Coherent manipulation of an Andreev spin qubit, Science **373**, 430 (2021).
[19] R. Aguado, A perspective on semiconductor-based superconducting qubits, Appl. Phys. Lett. **117**, 240501 (2020).
[20] F. W. J. Hekking and L. I. Glazman, Quantum fluctuations in the equilibrium state of a thin superconducting loop, Phys. Rev. B **55**, 6551 (1997).
[21] See Supplemental Material at http://link.aps.org/supplemental/10.1103/PhysRevB.110.L020504 for the details of the derivations, which includes Refs. [29–31].
[22] A. O. Caldeira and A. J. Leggett, Influence of dissipation on quantum tunneling in macroscopic systems, Phys. Rev. Lett. **46**, 211 (1981).
[23] G. Schön and A. Zaikin, Quantum coherent effects, phase transitions, and the dissipative dynamics of ultra small tunnel junctions, Phys. Rep. **198**, 237 (1990).
[24] G. Catelani, S. E. Nigg, S. M. Girvin, R. J. Schoelkopf, and L. I. Glazman, Decoherence of superconducting qubits caused by quasiparticle tunneling, Phys. Rev. B **86**, 184514 (2012).
[25] A. A. Abrikosov, L. P. Gorkov, and I. E. Dzyaloshinskii, *Methods of Quantum Field Theory in Statistical Physics* (Dover, New York, 1975).
[26] L. N. Bulaevskii, V. V. Kuzii, and A. A. Sobyanin, Superconducting system with weak coupling to the current in the ground state, JETP Lett. **25**, 290 (1977).
[27] P. D. Kurilovich, V. D. Kurilovich, V. Fatemi, M. H. Devoret, and L. I. Glazman, Microwave response of an Andreev bound state, Phys. Rev. B **104**, 174517 (2021).
[28] L. Fu and C. L. Kane, Superconducting proximity effect and Majorana fermions at the surface of a topological insulator, Phys. Rev. Lett. **100**, 096407 (2008).
[29] A. I. Larkin and Y. N. Ovchinnikov, Density of states in inhomogeneous superconductors, Sov. Phys. JETP **34**, 1144 (1972).
[30] M. V. Feigel'man and M. A. Skvortsov, Universal broadening of the Bardeen-Cooper-Schrieffer coherence peak of disordered superconducting films, Phys. Rev. Lett. **109**, 147002 (2012).
[31] S. K. Yip, Supercurrent and noise in point contacts between two different superconductors, Phys. Rev. B **68**, 024511 (2003).